THE JOURNAL OF PHYSICAL CHEMISTRY B

Article

pubs.acs.org/JPCB

Cis Carotenoids: Colorful Molecules and Free Radical Quenchers

Elizabeth Hernandez-Marin,*[,†] Annia Galano,*[,‡] and Ana Martínez[†]

[†]Instituto de Investigaciones en Materiales, Universidad Nacional Autónoma de México, Circuito Ext. s/n, Ciudad Universitaria, P.O. Box 70-360, Coyoacán, 04510 México, D. F. México

[‡]Departamento de Química, División de Ciencias Básicas e Ingeniería, Universidad Autónoma Metropolitana-Iztapalapa, San Rafael Atlixco 186, Col. Vicentina, Iztapalapa. A.P. 55-534, 09340, México DF, México

Supporting Information

ABSTRACT: We present a density functional theory (DFT) and time-dependent density functional theory (TD-DFT) study on the stability, antioxidant properties with respect to the single electron transfer mechanism, and electronic absorption spectra of some isomers (9-*cis*, 13-*cis*, and 15-*cis*) of carotenoids such as astaxanthin, lycopene, and those present in virgin olive oil (lutein, *β*-carotene, neoxanthin, antheraxanthin, violaxanthin, neochrome, luteoxanthin, mutatoxanthin, and violaxanthin). In general, the calculated relative stability of the *cis* isomers appears to be in line with experimental observations. It is predicted that the above-mentioned carotenoids (*cis* and *trans* isomers) will transfer one electron to the $^{\bullet}OH$ radical. However, this transference is not plausible with radicals such as $^{\bullet}OOH$, $^{\bullet}OC_2H_5$, $^{\bullet}OOC_2H_5$, $^{\bullet}NO_2$, and $^{\bullet}OOCH_2CH{=}CH_2$. On the other hand, some carotenoids (*β*-carotene, lycopene, lutein, astaxanthin, violaxanthin, and antheraxanthin) will likely accept, in a medium of low polarity, one electron from the radical $^{\bullet}O_2^-$. However, neoxanthin, auroxanthin, mutatoxanthin, luteoxanthin, and neochrome would not participate in such an electronic transfer mechanism. The TD-DFT studies show that neutral species of the *cis* and *trans* isomers maintain the same color. On the contrary, the ionic species undergo a "bleaching" process where the absorption wavelengths shift to longer values (>700 nm). Additionally, the formation of a complex between astaxanthin and Cu^{2+} is explored as well as the effect that the metal atom will have in the UV−vis spectrum.

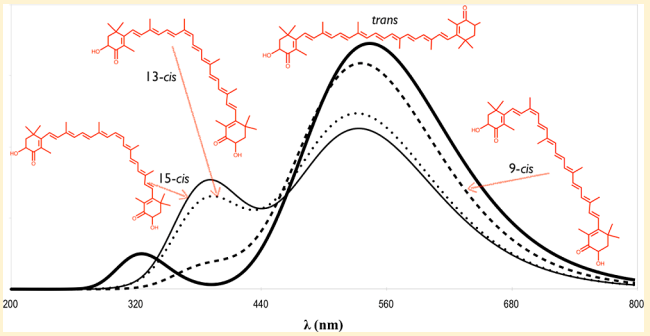

INTRODUCTION

Oxidative stress refers to the chemical damage that is produced by free radicals, or other oxidants, to molecules of high biological importance. Free radicals are very short-lived reactive molecules that injure proteins and nitrogen basis, producing numerous health disorders[1] such as Alzheimer,[2−6] atherosclerosis,[7−10] cancer,[11−14] and some cardiovascular problems.[15−19] One of the most common strategies to fight or prevent oxidative stress is using free radical scavengers. Carotenoids are well-known for their capacity to scavenge free radicals.[20,21] For many years, the nutritional function of carotenoids has been investigated and even now it is still of interest.[22−24] It has been established that mammals incorporate carotenoids through the diet and also that one of the main biological functions of these compounds is to act as precursors of Vitamin A.[25,26] In addition, there are other benefits related to the consumption of carotenoids in the diet, including their biological activities as antioxidants and some additional health benefits reducing the risk of some cardiovascular diseases and certain types of cancer.[27] This has increased the interest on these compounds, in particular on their potential role improving health through diet by consumption of foods rich in carotenoids.

Carotenoids contain a polyene chain that reacts with light, acids, heat, and oxygen.[28] As a consequence, carotenoids may show color loss, which is apparently related to a decrease in their biological activity.[29−31] Moreover, carotenoids in natural foods are mostly *trans* isomers, but they are susceptible to some *cis*−*trans* isomerization reactions during food processing.[32,33] Several authors have investigated the degradation products of carotenoids formed during heating,[34−39] and it has been proposed that the oxidation of carotenoids produces colorless compounds that might affect the flavor.[40,41] This is important because the color in foods is commonly related to the quality of the products. For example, the color of the virgin olive oil determines its price, and also indicates the characteristic of the flavor.[39] Some of the carotenoids present in virgin olive oils are lutein, *β*-carotene, neoxanthin, antheraxanthin, and violaxanthin.[38,39] Upon heating, some of these molecules may be transformed into related carotenoids such as neochrome (for neoxanthin), mutatoxanthin (for antheraxanthin), luteoxanthin, and auroxanthin (for violaxanthin).[39] In spite of the investigations concerning the degradation products of carotenoids, there is not much detailed information related to the antioxidant capacity of each isomer,[42] and there is only

Received: February 15, 2013
Revised: March 20, 2013
Published: April 5, 2013

Scheme 1. Schematic Representation of the *trans* Isomers of the Carotenoids under Study

Carotenoid (acronym)	Structure
all trans auroxanthin (*trans* AURO)	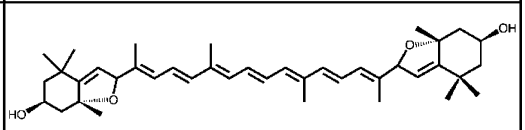
all trans luteoxanthin (*trans* LUTEO)	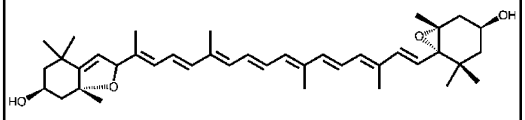
all trans neochrome (*trans* NEOCHR)	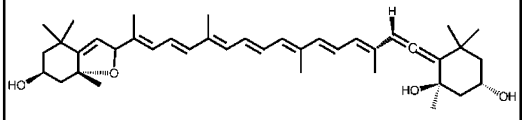
all trans mutatoxanthin (*trans* MUTATO)	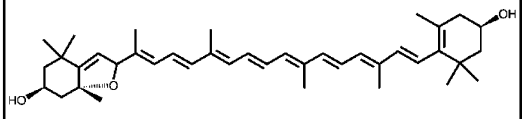
all trans neoxanthin (*trans* NEOX)	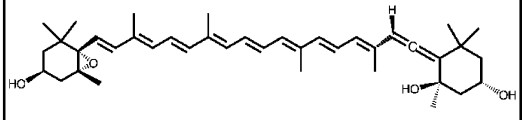
all trans violaxanthin (*trans* VIOLA)	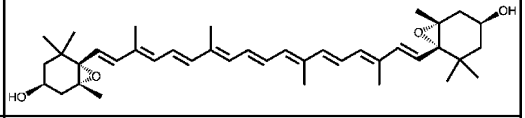
all trans antheraxanthin (*trans* ANTHER)	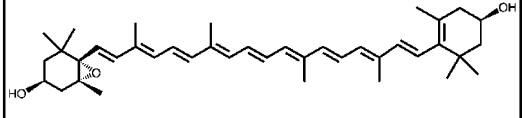
all trans lutein (*trans* LUT)	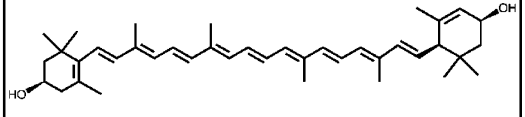
all trans β-carotene (*trans* BC)	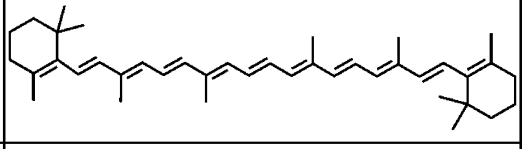
all trans lycopene (*trans* LYCO)	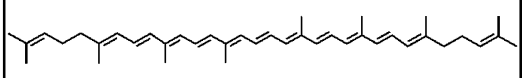
all trans astaxanthin (*trans* ASTA)	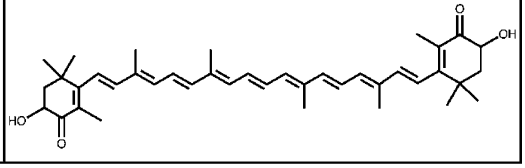

some available information on the color differences between the *cis* and all-*trans* isomers.[43,44]

It has been previously reported that some carotenoids are able to chelate metals and, as a consequence, the molecules absorb at longer wavelengths.[45,46] In one previous report,[47] some metal complexes with astaxanthin (M-ASTA) were studied theoretically. However, different conformers of these metal complexes were not considered. To complete that investigation, this report also includes results for some Cu–ASTA complexes in different conformations, since it might also be important to analyze the effect that the coordination with metals has on the color of carotenoids.

dx.doi.org/10.1021/jp401647n | *J. Phys. Chem. B* 2013, 117, 4050–4061

Scheme 2. Schematic Representation of the *5-cis* LYCO and the *9-cis*, *13-cis*, and *15-cis* LUT Isomers

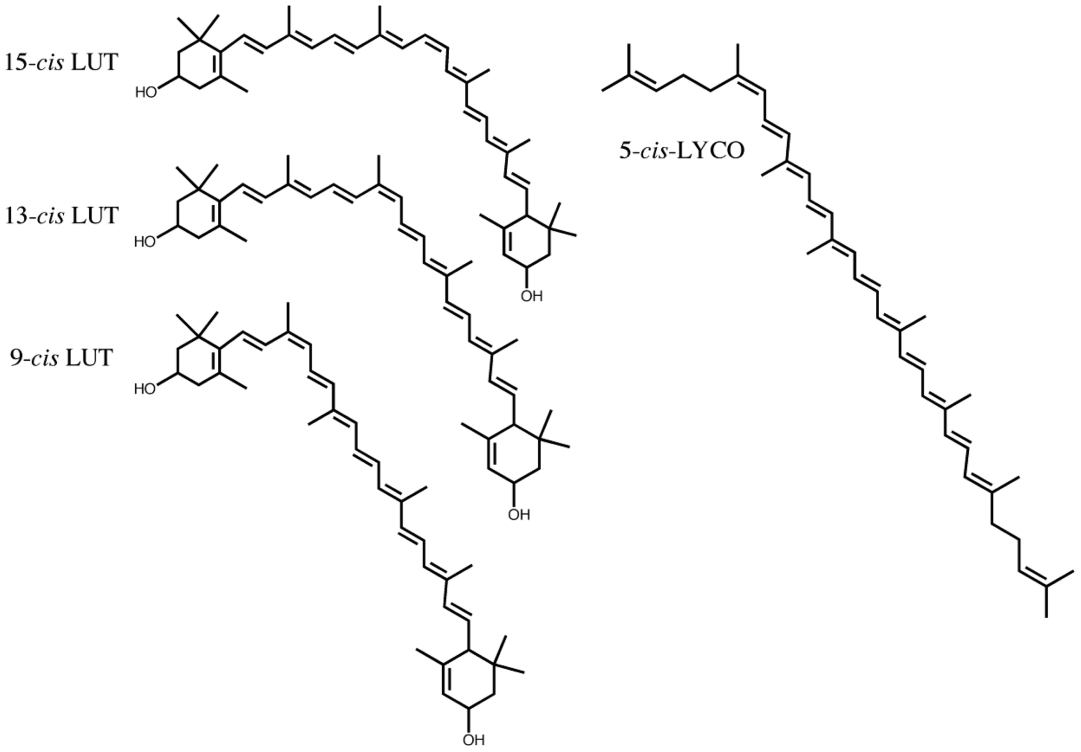

In summary, the main goal of this investigation is to analyze the antioxidant properties of the *cis* isomers of some carotenoids in comparison with the all-*trans* isomers, and also to study their electronic absorption properties. In addition, the potential role of metal complexation in such aspects is investigated.

COMPUTATIONAL DETAILS

Geometry optimizations and frequency calculations have been carried out using the B3LYP[48,49] functional in conjunction with the 6-31G(d) basis set. The energies were further improved by single point calculations using the 6-311+G(d,p) basis set. Solvent effects were included *a posteriori* by single point calculations using the polarizable continuum model, specifically the integral-equation-formalism (IEF-PCM)[50,51] and RADII = UFF, with the 6-311+G(d,p) basis set. These calculations have been performed using benzene and water as solvents, to mimic non-polar and polar environments, respectively. Unrestricted calculations were used for open shell systems. Local minima were identified by the absence of imaginary frequencies. All the electronic calculations were performed with the Gaussian 09 package of programs.[52] Thermodynamic corrections at 298.15 K were included in the calculation of relative energies. The electronic spectra have been computed using the time dependent density functional theory (TD-DFT), based on vertical excitations involving the six lowest lying excited states. Also, to assess the possible importance of long-range corrections on the quality of the calculated UV−vis spectra, this part of the investigation has been performed with the functionals B3LYP and CAM-B3LYP,[53] both with the 6-311+G(d,p) basis set.

RESULTS AND DISCUSSION

The carotenoids under study include those that are present in virgin olive oil. Additionally, lycopene and astaxanthin have also been taken into account. The structure of lycopene does not contain the β-ionone ring end of β-carotene.[54] Astaxanthin includes a keto moiety at its terminal rings, and it does not have any epoxide groups. These two carotenoids were considered here to investigate whether the structural changes produce a major effect on the properties under study, when compared to the carotenoids from olive oil. The schematic representations of all-*trans* isomers are shown in Scheme 1. In general, for each carotenoid, three *cis* isomers were considered (9-*cis*, 13-*cis*, and 15-*cis*). The presence of these isomers, especially 9-*cis* and 13-*cis*, has been identified in major vegetable crops.[23,34−37] It should be noted that, for lycopene, an additional *cis* isomer (5-*cis*) was studied. This isomer is commonly found in humans and also in vegetable tissues.[54] As an example, Scheme 2 contains the schematic representation of the three *cis* isomers for lutein, as well as the 5-*cis*-lycopene molecule. Finally, one additional conformation (to be referred to in this document as twist-ASTA) was incorporated into the study. The representation of the twist-ASTA conformation can be found in the Supporting Information.

1. Relative Stability of the Isomers. The results of the relative stability, in terms of the calculated Gibbs energy, and the relative Maxwell−Boltzmann population are reported in Table 1. In all cases, the 15-*cis* isomer is the less stable molecule. With one exception (the 13-*cis*-AURO molecule), the *trans* isomers are more stable than their corresponding 9- and 13-*cis* isomers by 0.24−2.85 kcal/mol. The relative Boltzmann population is related to the energy difference between the *cis* and the all-*trans* isomers, indicating that there are some carotenoids (NEOX, VIOLA, LUT, BC, LYCO, ASTA) that are mainly *trans* (a percent population larger than 70%). A

dx.doi.org/10.1021/jp401647n | J. Phys. Chem. B 2013, 117, 4050−4061

Table 1. Calculated Gibbs Energies (kcal/mol), Relative to the All-*trans* Isomer, in the Gas Phase (Gas), Benzene (Bz), and Water (Wt)[a]

	relative energy (kcal/mol)			Maxwell−Boltzmann population (%)		
carotenoids	Gas	Bz	Wt	Gas	Bz	Wt
trans-AURO	0.00	0.00	0.00	13.0	13.0	12.8
9-*cis*-AURO	0.24	0.26	0.32	8.7	8.4	7.5
13-*cis*-AURO	−1.03	−1.03	−1.05	73.7	73.9	75.0
15-*cis*-AURO	0.62	0.60	0.59	4.6	4.7	4.7
trans-LUTEO	0.00	0.00	0.00	65.1	66.5	68.3
9-*cis*-LUTEO	0.86	0.90	0.98	15.2	14.5	13.2
13-*cis*-LUTEO	0.78	0.81	0.85	17.6	16.8	16.3
15-*cis*-LUTEO	2.01	2.02	2.02	2.2	2.2	2.3
trans-NEOCHR	0.00	0.00	0.00	61.8	63.1	63.7
9-*cis*-NEOCHR	0.79	0.84	0.91	16.3	15.3	13.8
13-*cis*-NEOCHR	0.65	0.67	0.65	20.7	20.3	21.1
15-*cis*-NEOCHR	2.31	2.30	2.28	1.2	1.3	1.4
trans-MUTATO	0.00	0.00	0.00	45.4	47.3	52.4
9-*cis*-MUTATO	0.06	0.12	0.27	40.8	38.5	33.2
13-*cis*-MUTATO	0.82	0.84	0.89	11.3	11.5	11.6
15-*cis*-MUTATO	1.71	1.70	1.73	2.5	2.7	2.8
trans-NEOX	0.00	0.00	0.00	72.3	73.3	74.7
9-*cis*-NEOX	0.93	0.98	1.08	15.1	14.0	12.0
13-*cis*-NEOX	1.10	1.11	1.09	11.2	11.3	11.8
15-*cis*-NEOX	2.35	2.33	2.32	1.4	1.4	1.5
trans-VIOLA	0.00	0.00	0.00	95.5	95.7	96.3
9-*cis*-VIOLA	1.99	2.03	2.16	3.3	3.1	2.5
13-*cis*-VIOLA	2.85	2.85	2.84	0.8	0.8	0.8
15-*cis*-VIOLA	3.32	3.30	3.27	0.4	0.4	0.4
trans-ANTHER	0.00	0.00	0.00	54.2	55.3	56.7
9-*cis*-ANTHER	1.48	1.53	1.63	4.4	4.2	3.6
13-*cis*-ANTHER	0.17	0.19	0.22	40.9	40.0	39.2
15-*cis*-ANTHER	2.79	2.78	2.77	0.5	0.5	0.5
trans-LUT	0.00	0.00	0.00	90.1	90.3	90.4
9-*cis*-LUT	1.39	1.41	1.41	8.6	8.4	8.3
13-*cis*-LUT	2.61	2.62	2.64	1.1	1.1	1.1
15-*cis*-LUT	3.68	3.66	3.65	0.2	0.2	0.2
trans-BC	0.00	0.00	0.00	71.2	71.5	71.2
9-*cis*-BC	1.20	1.21	1.20	9.4	9.3	9.3
13-*cis*-BC	0.85	0.87	0.85	16.9	16.6	16.8
15-*cis*-BC	1.98	1.96	1.95	2.5	2.6	2.6
trans-LYCO	0.00	0.00	0.00	92.1	92.3	92.4
5-*cis*-LYCO	2.17	2.23	2.34	2.4	2.2	1.8
9-*cis*-LYCO	2.11	2.12	2.12	2.6	2.6	2.6
13-*cis*-LYCO	2.15	2.13	2.07	2.4	2.5	2.8
15-*cis*-LYCO	3.19	3.17	3.14	0.4	0.4	0.5
trans-ASTA	0.00	0.00	0.00	79.9	80.8	81.0
9-*cis*-ASTA	1.38	1.46	1.56	7.8	6.9	5.9
13-*cis*-ASTA	1.25	1.26	1.24	9.7	9.6	10.1
15-*cis*-ASTA	2.01	2.02	1.95	2.7	2.7	3.0

[a]The Maxwell−Boltzmann population is also included.

smaller predominance of the *trans* isomers occurs with LUTEO and NEOCHR (65.1 and 61.8%, respectively). There are other cases in which the probability of having the *trans* and one *cis* isomer is similar. For example, the population of *trans*-MUTATO is 45.4% versus 40.8% for 9-*cis*-MUTATO. A similar situation appears with the *trans*- and 13-*cis*-ANTHER isomers (54.2 and 40.9%, respectively). The results in Table 1 show that 13-*cis*-AURO is more stable than the *trans* isomer by 1.03 kcal/mol. As a consequence, the population of 13-*cis*-AURO is calculated to be 73.7%.

For LUTEO, NEOCHR, ANTHER, BC, and ASTA, the stability order is *trans* > 13-*cis* > 9-*cis* > 15-*cis*. For ASTA and BC, these results are in line with experimental findings.[55−57] In the case of MUTATO, NEOX, VIOLA, and LUT, the 9-*cis* isomer is more stable than the 13-*cis* species. According to the experimental information,[35] the predominant *cis* isomer of LUT in fresh vegetables is 13-*cis*-LUT. Apparently, in this instance, the theoretical results are not in agreement with the experimental findings, since the 9-*cis* isomer was found to be more stable for LUT. Thus, the predominance of 13-*cis*-LUT in fresh vegetables may be related with other conditions rather than stability.

At the Hartree−Fock level of theory,[58] 5-*cis*-LYCO was found to be more stable than *trans*-LYCO by 0.4 kcal/mol. On the contrary, in the present work (DFT), 5-*cis*-LYCO is less stable than *trans*-, 9-*cis*-, and 13-*cis*-LYCO. These results indicate that the correlation included in the DFT calculations is important for the description of the stability of these molecules. Experimental observations on tomato extracts[59] show that *trans*-LYCO is the most stable species, followed by 5-*cis*-, 13-*cis*-, and 9-*cis*-LYCO. Our results are in agreement with these experimental results, concerning the most stable species, but there is an apparent contradiction regarding the *cis* isomers. In any case, the energy differences between the *cis* isomers are very small, and it is not possible to definitively conclude which one is the most stable.

For AURO, the calculated relative stability is 13-*cis*-AURO < *trans*-AURO < 9-*cis*-AURO < 15-*cis*-AURO (Table 1). Experimental studies on kiwi fruits[60] imply that *trans*-AURO is the most stable species. Considering that the calculated energy differences between the most stable and the next species are about 1 kcal/mol, it can be proposed that the computing of the thermodynamic terms (for example, the thermal correction to Gibbs free energy) will give rise to the slight discrepancies between the experimental observations and the theoretical results in Table 1. It is important to note that all energy differences reported in Table 1 are very small (lower than 3.5 kcal/mol, i.e., within the accuracy of calculations) and caution is required to affirm that one isomer is more stable than the other. In general, the theoretical results can be deemed in acceptable agreement with the experimental observations.

2. Single Electron Transfer (Antiradical Capacity). One reaction mechanism related to the free radical scavenging activity of carotenoids is the single electron transfer reaction (SET) mechanism.[20,21] The vertical ionization energy (VIE) and the vertical electron affinity (VEA) have been successfully applied to the study of this mechanism.[61−63] Some of the theoretical results reported so far were in line with previous observations (for the case of the $^{\bullet}$OOH radical),[64] and other predictions (for the case of the reaction with the radical $^{\bullet}$OH) have been validated experimentally.[65] The use of a full electron donator acceptor map (FEDAM),[61,62] which is the graphic representation of the coordinate pair (VEA, VIE), allows for a qualitative identification of the relative electron-donor or electron-acceptor capability among the molecules that are included in the map. Qualitatively, the electrons will be transferred from species located at the lower left of the map to species located at the upper right (lower-left to upper-right electron transference).

Figure 1 shows the FEDAMs in two environments of very different polarity, benzene and water. To illustrate the

dx.doi.org/10.1021/jp401647n | J. Phys. Chem. B 2013, 117, 4050−4061

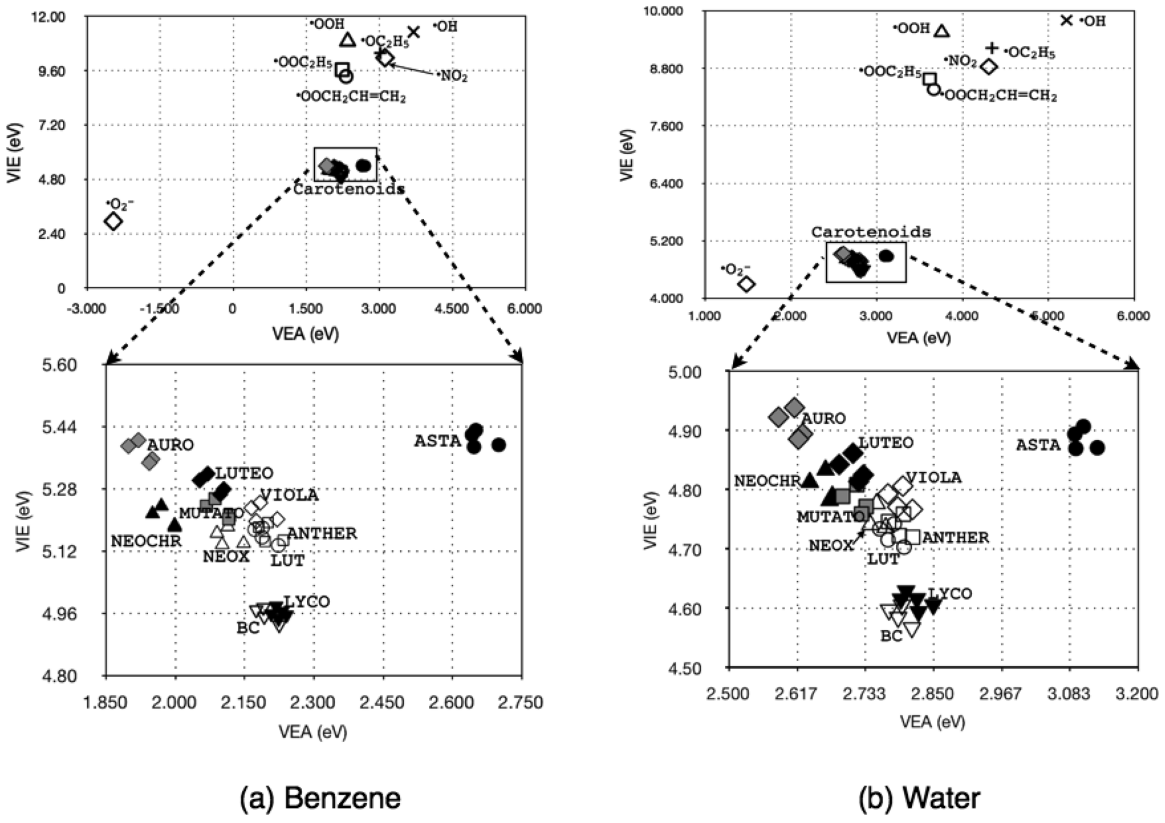

Figure 1. FEDAM in (a) benzene and (b) water containing the *cis* and *trans* carotenoid isomers as well as some free radicals.

qualitative use of the FEDAM, besides all the *cis*–*trans* isomers considered in this study, some representative free radicals such as $^{\bullet}OH$, $^{\bullet}OOH$, $^{\bullet}O_2^-$, $^{\bullet}OC_2H_5$, $^{\bullet}OOC_2H_5$, $^{\bullet}NO_2$, and $^{\bullet}OOCH_2CH{=}CH_2$ are also included in these maps. Following the "lower-left to upper-right electron transference" described above, it can be seen that the peroxide radical ($^{\bullet}O_2^-$) will preferably transfer one electron to the carotenoids. For BC, ASTA, LUT, and LYCO, quantitative theoretical calculations predicted that this transference will occur in benzene but not in water.[66] Likewise, carotenoids could in principle transfer one electron to the radicals located up to the right in the FEDAM. Previous theoretical studies predicted that $^{\bullet}OH$ would accept one electron from some carotenoids such as BC and ASTA, in water but not in benzene,[63] and that the electron transference between BC or ASTA and any of the free radicals $^{\bullet}OOH$, $^{\bullet}OC_2H_5$, and $^{\bullet}OOC_2H_5$ was very unlikely to occur, regardless of the environment's polarity. In line with those previous results[63,66] and from the FEDAM in Figure 1, it can be proposed that all the *cis* and *trans* isomers will transfer one electron to $^{\bullet}OH$ in water. In contrast, the occurrence of a single electron transfer (SET) between any of the carotenoids in Figure 1 and $^{\bullet}OOH$, $^{\bullet}OC_2H_5$, $^{\bullet}OOC_2H_5$, $^{\bullet}NO_2$, or $^{\bullet}OOCH_2CH{=}CH_2$ is not likely to occur. With respect to the reactivity toward $^{\bullet}O_2^-$, in addition to all the isomers of BC, LYCO, LUTE, and ASTA, the *trans* and *cis* species of VIOLA and ANTHER will likely accept one electron from $^{\bullet}O_2^-$ in benzene. This is because their VEA values are very similar. The other carotenes (NEOX, AURO, MUTATO, LUTEO, and NEOCHR) are not likely to accept an electron from $^{\bullet}O_2^-$ because they are located to the left of BC (at smaller values than the VEA of BC). Therefore, they are worse electron acceptors than BC. The theoretical values of VEA and VIE can be found in the Supporting Information.

It has been noted that 9-*cis*-ASTA apparently shows a higher antioxidant activity than the *trans* isomer.[67] Further, Levin and Mokady[68] reported that 9-*cis*-BC has a higher antioxidant potency *in vitro* than the *trans*-BC species. On the contrary, Mueller and Boehm[42] reported that BC shows a nonsignificant dependence between the position of the *cis* double bond and the antioxidant activity. It can be seen in Figure 1 that the values of VIE and VEA differ by no more than 0.1 eV for each isomer of the same carotenoid (for the case of BC, the values plotted here are in good agreement with those reported by Cerezo and co-workers[69]). Thus, it is expected that the antioxidant capabilities, regarding the SET reaction, of the *cis* isomers will not drastically change with respect to those of their respective *trans* species. Further experimental studies may help to determine the antiradical capacity of the *cis* isomers.

3. UV–vis. The hybrid functional B3LYP has been successfully used to study the UV–vis spectra of carotenoids.[70] While it has been stated that this functional produces very low carotenoid excitation energies,[71] B3LYP qualitatively reproduces the experimental trends.[70] The use of the long-range corrected version of B3LYP (CAM-B3LYP) has shown a good agreement with experimental measurements.[72] Table 2 shows the wavelengths of maximum absorption (λ_{max}) calculated with the functionals B3LYP and CAM-B3LYP in the gas phase and in benzene. It can be seen that CAM-B3LYP improves the agreement between calculated and experimental results with respect to the results obtained with the B3LYP functional. Therefore, from now on, the analysis of the spectra will be performed on the basis of the CAM-B3LYP results. It should be noted, however, that with both functionals the same

dx.doi.org/10.1021/jp401647n | J. Phys. Chem. B 2013, 117, 4050–4061

Table 2. UV−vis Maximum Absorption Wavelength (λ_{max}) in nm, Calculated in Benzene (Bz) and the Gas Phase (Gas) with the Functional B3LYP and CAM-B3LYP[a]

		theoretical λ_{max}				% contrib.	% error λ_{max}	
		B3LYP		CAM-B3LYP			B3LYP	CAM-B3LYP
carotenoids	Exp[b] λ_{max}	Gas	Bz	Gas	Bz	H → L transition	Bz	Bz
trans-AURO	400	467	503	418	446	96.3	25.8	11.5
9-*cis*-AURO		468	503	419	446	96.3		
13-*cis*-AURO		463	496	413	439	96.2		
15-*cis*-AURO		467	499	416	444	96.5		
trans-LUTEO	420	503	543	444	474	95.3	29.3	12.9
9-*cis*-LUTEO		504	544	445	475	95.3		
13-*cis*-LUTEO		499	536	439	467	95.1		
15-*cis*-LUTEO		502	539	441	469	95.4		
trans-NEOCHR	422	501	540	443	472	95.3	28.0	11.9
9-*cis*-NEOCHR		502	542	443	473	95.2		
13-*cis*-NEOCHR		496	533	436	464	95.0		
15-*cis*-NEOCHR		500	536	439	466	95.4		
trans-MUTATO	426	519	560	454	484	94.6	31.5	13.6
9-*cis*-MUTATO		520	562	455	486	94.5		
13-*cis*-MUTATO		514	552	448	475	94.3		
15-*cis*-MUTATO		518	556	450	479	94.2		
trans-NEOX	438	536	580	468	499	94.2	32.4	13.9
9-*cis*-NEOX		530	572	463	493	94.2		
13-*cis*-NEOX		533	571	461	489	93.9		
15-*cis*-NEOX		535	574	462	493	94.3		
trans-VIOLA	440	538	582	469	501	94.3	32.3	13.9
9-*cis*-VIOLA		532	575	464	495	94.3		
13-*cis*-VIOLA		534	573	462	491	94.0		
15-*cis*-VIOLA		537	566	465	494	94.3		
trans-ANTHER	445	553	598	477	509	93.6	34.3	14.4
9-*cis*-ANTHER		547	590	473	504	93.6		
13-*cis*-ANTHER		547	590	470	499	93.3		
15-*cis*-ANTHER		552	592	473	502	93.6		
trans-LUT	445	553	599	477	501	93.6	34.6	12.6
9-*cis*-LUT		545	589	471	503	93.6		
13-*cis*-LUT		548	589	470	500	93.3		
15-*cis*-LUT		552	593	474	503	93.6		
trans-BC	454	595	648	504	540	92.1	42.7	18.9
9-*cis*-BC		586	637	497	532	92.1		
13-*cis*-BC		589	639	496	528	91.6		
15-*cis*-BC		593	641	499	532	92.0		
trans-LYCO	470	590	635	490	520	89.3	35.1	10.6
5-*cis*-LYCO		589	634	488	518	89.0		
9-*cis*-LYCO		600	646	497	527	88.2		
13-*cis*-LYCO		609	657	506	535	89.3		
15-*cis*-LYCO		612	657	509	538	90.0		
trans-ASTA	470	605	661	508	544	90.6	40.6	15.7
9-*cis*-ASTA		600	653	501	536	90.5		
13-*cis*-ASTA		602	651	500	533	90.0		
15-*cis*-ASTA		602	652	502	534	90.6		

[a]The TDDFT percent contribution to the excitation from the HOMO → LUMO (H → L) transition is included. [b]The experimental values correspond to measurements made in hexane for the *trans* isomers included in ref 44.

experimental trends (regarding the increase of the values of λ_{max} from one carotenoid to another) are maintained. For all the molecules under study, the excitation with the largest oscillator strength (intensity) corresponds to a $\pi-\pi^*$ (HOMO−LUMO) transition. The TDDFT calculations indicate that this HOMO−LUMO transition is the major contribution (values ranging from 89% for 5-*cis*-LYCO to 96.5% for 15-*cis*-AURO) to the calculated excitation. Table 2 also includes the calculated percent contribution to the excitation from the HOMO−LUMO (H → L) transition.

The presence of carotenoid *cis* isomers can be established when the UV−vis spectrum presents an absorption band (*cis* peak) around 142 nm below the λ_{max} of the *trans* isomer.[44] The *cis* peaks are correctly reproduced by the TDDFT calculations. Table 3 includes the results for the wavelengths of the 13- and 15-*cis* isomers, which are the species where the *cis* peak is most intense. It can be seen that B3LYP in benzene fails to reproduce

dx.doi.org/10.1021/jp401647n | J. Phys. Chem. B 2013, 117, 4050−4061

Table 3. 13- and 15-*cis* Maximum Absorption Wavelength ($\lambda_{cis\ max}$) in nm for the Simulated *cis* Peak in Benzene (Bz) and the Gas Phase (Gas) with the Functional B3LYP and CAM-B3LYP[a]

	theoretical $\lambda_{cis\ max}$				λ_{theo}			
	B3LYP		CAM-B3LYP		CAM-B3LYP			
carotenoid *cis* isomers	gas	Bz	gas	Bz	gas	transition	% contrib.	approx.[b] λ_{cis}
13-*cis*-AURO	308	322	282	300	282	H → L + 1	76.0	283
						H − 1 → L	20.3	
15-*cis*-AURO	303	318	281	300	280	H → L + 1	78.7	
						H − 1 → L	17.9	
13-*cis*-LUTEO	332	349	299	333	299	H → L + 1	88.4	299
						H − 1 → L	6.5	
15-*cis*-LUTEO	327	347	301	320	299	H → L + 1	85.2	
						H − 1 → L	10.8	
13-*cis*-NEOCHR	330	ND	299	317	297	H → L + 1	88.3	308
						H − 1 → L	6.0	
15-*cis*-NEOCHR	325	349	299	319	297	H → L + 1	85.7	
						H − 1 → L	9.7	
13-*cis*-MUTATO	354	ND	311	331	318	H − 1 → L	91.9	314
					306	H → L + 1	91.2	
15-*cis*-MUTATO	352	367	311	333	322	H − 1 → L	90.4	
					307	H → L + 1	90.7	
13-*cis*-NEOX	352	ND	319	340	317	H → L + 1	89.5	325
						H − 1 → L	4.7	
15-*cis*-NEOX	346	ND	317	344	313	H → L + 1	89.7	
						H − 1 → L	4.8	
13-*cis*-VIOLA	354	375	318	343	318	H → L + 1	89.2	323
						H − 1 → L	5.2	
15-*cis*-VIOLA	349	365	316	344	316	H → L + 1	88.9	
						H − 1 → L	6.0	
13-*cis*-ANTHER	375	ND	330	351	334	H − 1 → L	91.0	330
					323	H → L + 1	90.5	
15-*cis*-ANTHER	372	ND	330	353	337	H − 1 → L	91.1	
					323	H → L + 1	91.4	
13-*cis*-LUT	370	390	326	353	335	H − 1 → L	91.1	335[c]
					325	H → L + 1	91.5	
15-*cis*-LUT	357	390	330	354	338	H − 1 → L	91.1	
					323	H → L + 1	91.4	
13-*cis*-BC	392	422	350	381	358	H − 1 → L	87.6	330[c]
					341	H → L + 1	4.3	
						H → L + 1	86.0	
						H − 1 → L	6.2	
15-*cis*-BC	390	420	350	382	360	H − 1 → L	90.1	
					340	H − 2 → L + 1	5.9	
						H → L + 1	89.1	
						H − 1 → L + 2	6.3	
13-*cis*-LYCO	409	ND	367	398	367	H → L + 1	34.1	360[c]
						H − 1 → L	60.0	
15-*cis*-LYCO	ND	443	365	396	365	H → L + 1	31.7	362[c]
						H − 1 → L	62.4	
13-*cis*-ASTA	420	447	365	391	365	H → L + 1	63.5	NA
						H − 1 → L	24.4	
						H − 1 → L + 2	5.2	
15-*cis*-ASTA	418	447	362	389	363	H → L + 1	57.4	
						H − 1 → L	30.3	
						H − 1 → L + 2	5.0	

[a]The theoretical wavelengths λ_{theo} (gas phase, CAM-B3LYP) that make up the *cis* band as well as their respective transitions with percent contribution to the excitation are also listed. [b]The approximated λ_{cis} was calculated, following Britton,[44] at 142 nm below the longest-wavelength absorption maximum (the so-called band III) in the spectrum of the *trans* compound. NA: not applicable, band III not reported. ND: not determined, no excitation was obtained. [c]Experimental values from ref 32.

such a peak for the 13-*cis* isomers of NEOCHR, MUTATO, NEOX, ANTHER, and LYCO as well as for the 15-*cis* isomers of NEOX and ANTHER. In contrast, CAM-B3LYP reproduces the *cis* peak in all cases. Table 3 also shows that in some

dx.doi.org/10.1021/jp401647n | J. Phys. Chem. B 2013, 117, 4050−4061

instances, like with MUTATO, ANTHER, LUT, LYCO, and BC, the *cis* peak is made up of two excitations calculated at different wavelengths. In the rest of the cases, only one excitation gives rise to the *cis* peak. In general, the main contributions to the *cis* peak excitations involve HOMO−1 to LUMO or HOMO to LUMO+1 transitions (Table 3).

In addition to the appearance of the *cis* peak, some of the additional features that characterize the UV−vis spectrum of a *cis* isomer are a small displacement of λ_{max} to shorter wavelengths and a significant decrement in absorbance at λ_{max}.[44] In Figure 2, the simulated UV−vis spectra of the four

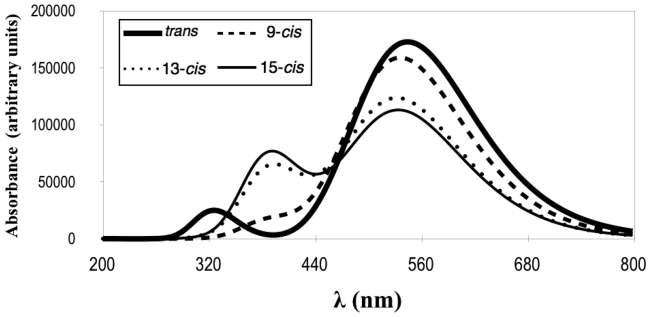

Figure 2. Simulated UV−vis spectra (CAM-B3LYP in benzene) for the all-*trans*- and *cis*-ASTA isomers. The appearance of the *cis* peak (around 400 nm) is more evident for the 13- and 15-*cis* species.

isomers of ASTA are shown to illustrate that these characteristics are well reproduced theoretically. Because the absorption wavelengths of the *cis* and *trans* isomer are very similar, it can be said that the isomerization process does not change the color of the carotenoids.

It has been reported[42] that, when carotenoids are exposed to radicals or oxidizing species, they undergo a "bleaching" process. The radical cations would absorb in the near-IR region (around 900−1000 nm),[74,75] and the radical anions are also expected to absorb in the near-IR region.[75] The radical anion BC$^{\bullet-}$ absorbs around 880 nm.[65] Table 4 presents the CAM-B3LYP values of the λ_{max}, both in the gas phase and in benzene, calculated for the anionic (*trans*-CAR$^{\bullet-}$) and cationic (*trans*-CAR$^{\bullet+}$) radical species of all the *trans* isomers. This table

Table 4. Experimental (When Available, from ref 74) and Theoretical[a] Maximum Absorption Wavelength (λ_{max}) in nm for the *trans* Radical Anions and Cations in the Gas Phase and Benzene

	gas		benzene		Exp. benzene
carotenoids	anion	cation	anion	cation	cation
trans-AURO	620	664	700	760	
trans-LUTEO	684	732	788	848	
trans-NEOCHR	674	730	766	852	
trans-MUTATO	714	786	826	924	
trans-NEOX	734	796	852	936	
trans-VIOLA	744	797	876	932	
trans-ANTHER	772	860	916	1024	
trans-LUT	772	860	916	1028	950
trans-BC	844[b]	968	1008	1220	1020
trans-LYCO	956	984	1176	1250	1050
trans-ASTA	1092	864	1500	1004	920

[a]CAM-B3LYP calculations. [b]Radical anion BC$^{\bullet-}$ is expected to absorb around 880 nm.[65]

also includes the experimentally measured[74] wavelengths for some cationic radical carotenoids.

Previous theoretical calculations[61] on ASTA, LYCO, LUT, and VIOLA, among other cationic radical carotenoids, carried out with the B3LYP functional gave very similar values. Here, the λ_{max} values calculated in benzene are overestimated by 10% (LUT and ASTA) and 20% (BC and LYCO) with respect to the available experimental values. When the gas phase results are considered instead, this error is no more than 10% in all cases. As an example, Figure 3 presents the simulated UV−vis spectra (in benzene) of the radical anion *trans*-LUTEO$^{\bullet-}$ and radical cation *trans*-LUTEO$^{\bullet+}$.

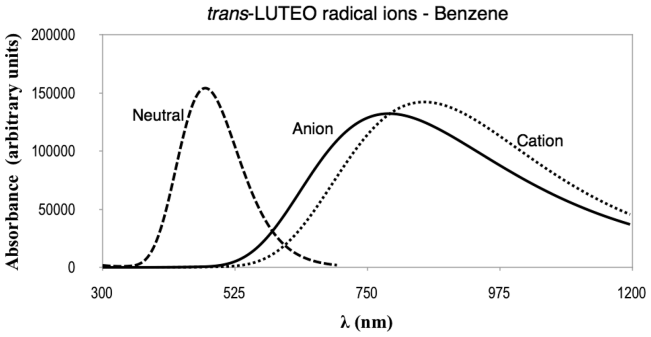

Figure 3. Simulated UV−vis spectra (CAM-B3LYP in benzene) for the radical cation and anion *trans*-LUTEO. The calculated λ_{max} shifts from 544 nm (neutral species) to about 700 and 760 nm, respectively. With the exception of ASTA, all of the calculated values of λ_{max} for the other carotenoids under study follow the same trend.

Figure 4 shows the molecular orbital diagram for the neutral, cationic, and anionic species of *trans*-LUTEO and *trans*-ASTA. When the cationic species is formed, the energy of the orbitals decreases with respect to those of the neutral species. Conversely, the formation of the anion increases the energy of the orbitals. In an unrestricted calculation, upon the formation of the cation, the HOMO "splits" into the α-spin highest singly occupied molecular orbital (αHSOMO) and the β-spin lowest singly unoccupied molecular orbital (βLSUMO). When the anionic species is formed, it is the LUMO that "splits" into the αHSOMO and the βLSUMO (see Figure 4). The TDDFT calculations indicate that the main contribution to the band with the maximum absorption in the spectra of the ions arises primarily from the βHSOMO → βLSUMO and αHSOMO → αLSUMO transitions (see Tables S2 and S3 in the Supporting Information).

Overall, according to the diagrams in Figure 4, the energy gap between the β-spin HSOMO and LSUMO in the ionic species decreases relative to the value of ΔE between the LUMO and HOMO in the neutral species. With the exception of ASTA, the (βLSUMO − βHSOMO) difference is slightly smaller for the cation than it is for the anion. Therefore, the cations absorb at longer wavelengths than the anions, for all the studied carotenoids, except ASTA. In this particular case, it is found that the energy difference between the β-spin LSUMO and HSOMO is larger for the cation (Figure 4). Consequently, the cation absorbs at shorter wavelengths than the anion. It should be noted that the presence of the keto group may play a role by increasing the conjugation and allowing a distribution of the charge in the anionic species. Thus, the destabilization of the LUMO is not so pronounced as in the cases of the other carotenes. The representations of the anionic βHSOMO and

dx.doi.org/10.1021/jp401647n | J. Phys. Chem. B 2013, 117, 4050−4061

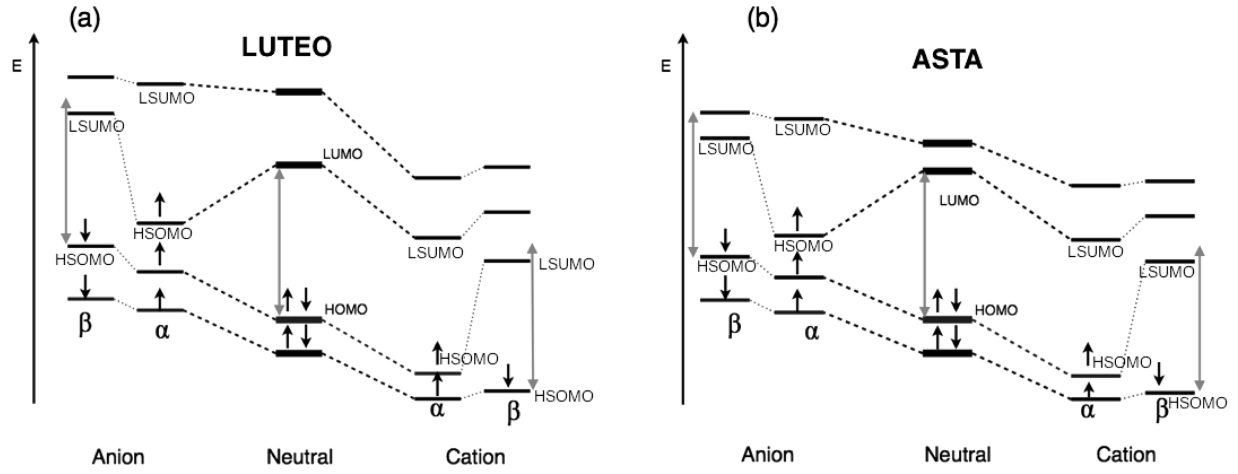

Figure 4. Molecular orbital diagram for the neutral, cationic, and anionic species of (a) *trans*-LUTEO and (b) *trans*-ASTA. Overall, the energy gap between the HSOMO and LSUMO in the ions decreases relative to the ΔE between the HOMO and LUMO in the neutral species (gray double ended arrow). (a) The ΔE between the βLSUMO and βHSOMO in the anions is slightly larger than the corresponding difference in the cation. (b) ASTA is the only case where the energy difference between the βLSUMO and βHSOMO is smaller for the anion than the corresponding difference for the cation.

βLSUMO of ASTA and LUTEO are included in the Supporting Information.

3. Metal–ASTA Complexes. The cation Cu^{2+} is considered to induce *cis*–*trans* isomerization in astaxanthin.[73] It was observed that, over time, the interaction of Cu(II) with *trans*-astaxanthin caused the maximum absorbance, at 480 nm, to decrease significantly, while the absorbance at 373 nm, which is characteristic of *cis* isomers of astaxanthin, gradually increased.[73] Polyakov et al.[46] noted that the mixture of astaxanthin and $CuCl_2$ in methylene chloride gave rise to a UV–vis spectrum where an additional band appears at 878 nm. They attributed this new absorption band to the presence of carotenoid radical cations, rather than to the formation of a metal complex. However, Figure 5 shows that an absorption at

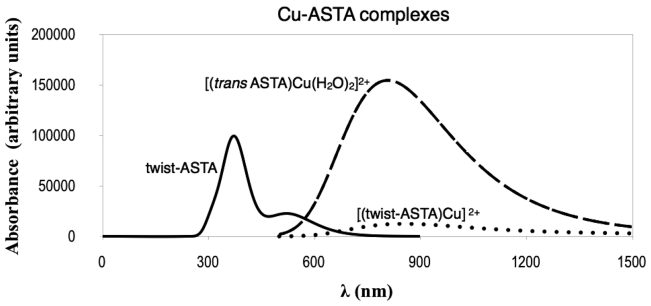

Figure 5. Simulated UV–vis spectra of the [(*trans*-ASTA)Cu-$(H_2O)_2]^{2+}$ complex, a *cis*-like conformation of astaxanthin (twist-ASTA) that may act as a tetradentate ligand, and the [(twist-ASTA)Cu]$^{2+}$ complex.

808 nm was calculated in the gas phase for the complex [(*trans*-ASTA)$Cu(H_2O)_2]^{2+}$. Therefore, it could be proposed that the experimental band observed at 878 nm might correspond to a Cu–(*trans*-ASTA) complex.

Thus, while Cu^{2+} induces *cis*–*trans* isomerization of astaxanthin, the additional formation of the metal complex cannot be completely overruled. To probe the plausibility of the complex formation, the Gibbs free energy of the following reaction was calculated:

$$[Cu(H_2O)_4]^{2+} + \textit{trans}\text{-ASTA} \rightarrow [(\textit{trans}\text{-ASTA})Cu(H_2O)_2]^{2+} + 2H_2O$$

This process is predicted to be exergonic, with $\Delta G = -78.8$ kcal/mol. Since such a value is much larger than any uncertainty inherent to calculations, the viability of the complexation process is proved. However, it is possible that the rate constant of the complex formation is smaller than the rate constant of the isomerization process. In any case, according to the features of the UV–vis spectra of *cis* isomers and those of the complexes, it can be concluded that the band around 880 nm corresponds to a copper–astaxanthin complex rather than to a *cis* isomer.

Due to the structure of astaxanthin, it could act as a tetradentate ligand if the molecule is twisted (see the schematic representation of such a conformation in the Supporting Information). This twisted conformation (that will be referred to as twist-ASTA) could be considered as a multiple *cis*-like conformer. Its simulated UV–vis spectrum is shown in Figure 5, and it presents one intense band at 349 nm. This band is located in the region where the *cis* peaks appear; suggesting that the presence of several *cis* regions would increase the intensity of this band. With respect to the stability of this species, twist-ASTA is about 20 kcal/mol less stable than the all-*trans*-ASTA. However, the stabilization of the twisted conformer can be assisted by the presence of a Cu^{2+} cation. This hypothesis is confirmed with the results obtained from our calculations, since the formation of this metal complex is favorable by 76 kcal/mol. Therefore, a net ΔG value of −56 kcal/mol would correspond to the overall process starting with all-*trans*-ASTA and ending with the tetra-coordinate [(twist-ASTA)Cu]$^{2+}$ chelate. Unfortunately, the presence of such a complex (that definitely would exist in a very small proportion) could not be detected via UV–vis spectroscopy because the simulated spectrum which appears in Figure 5 shows a negligible intensity all along the spectra. The representations of [(*trans*-ASTA)-$Cu(H_4O)_2]^{2+}$ and [(twist-ASTA)Cu]$^{2+}$ are also included in the Supporting Information.

dx.doi.org/10.1021/jp401647n | J. Phys. Chem. B 2013, 117, 4050–4061

CONCLUDING REMARKS

In general, the calculated relative stability of the *cis* isomers appears to be in line with experimental observations. Since the calculated Gibbs energy difference in many cases is around 1 kcal/mol, it is expected that in some instances one isomer would appear to be slightly more stable with respect to the other. This is especially evident in the case of the 9- and 13-*cis* isomers. In all cases, the 15-*cis* isomers were calculated to be the least stable ones. Experimentally, this isomer is seldom observed.

The antiradical properties of the *cis* isomers regarding the mechanism of electron transfer are moderately, if at all, modified with respect to the antiradical properties of the *trans* species. Thus, the *cis* isomers are as colorful and as good antiradicals as their *trans* counterparts.

One possibility for the carotenoids to lose their color is by reduction or oxidation via a single electron transfer mechanism. The radical ionic species absorb at long wavelengths (>700 nm). With the exception of *trans*-ASTA, the anions absorb at shorter wavelengths than the cationic species. Further, in the case of astaxanthin, another way to lose its color could be due to the formation of a coordination complex with Cu^{2+}.

ASSOCIATED CONTENT

Supporting Information

VEA and VIE in benzene and water of all the isomers, optimized structures of the twist-ASTA conformation, [(*trans*-ASTA)Cu$(H_2O)_2]^{2+}$, and [(twist-ASTA)Cu]$^{2+}$, representation of βLSUMO and βHSOMO for LUTEO and ASTA, and nature of the transitions that give rise to the bands of maximum absorption for the spectra of the ionic species. This material is available free of charge via the Internet at http://pubs.acs.org.

AUTHOR INFORMATION

Corresponding Author

*E-mail: ehdzmarin@gmail.com (E.H.-M.); agal@xanum.uam.mx (A.G.).

Notes

The authors declare no competing financial interest.

ACKNOWLEDGMENTS

This work was carried out using the KanBalam supercomputer, provided by DGTIC, UNAM, and the Laboratorio de Visualización y Cómputo Paralelo at Universidad Autónoma Metropolitana-Iztapalapa. This work was partially supported by project SEP-CONACyT 167491. E.H.-M. acknowledges the economic support of the Program of Postdoctoral Scholarships from DGAPA (UNAM). We thank M. Avelar and Y. Romero for their work on the initial calculations of some carotenoids.

REFERENCES

(1) Uttara, B.; Singh, A. V.; Zamboni, P.; Mahajan, R. T. Oxidative Stress and Neurodegenerative Diseases: A Review of Upstream and Downstream Antioxidant Therapeutic Options. *Curr. Neuropharmacol.* **2009**, *7*, 65−74.

(2) Butterfield, D. A.; Hensley, K.; Harris, M.; Mattson, M.; Carney, J. β-Amyloid Peptide Free Radical Fragments Initiate Synaptosomal Lipoperoxidation in a Sequence-Specific Fashion: Implications to Alzheimer's Disease. *Biochem. Biophys. Res. Commun.* **1994**, *200*, 710−715.

(3) Hensley, K.; Carney, J. M.; Mattson, M. P.; Aksenova, M.; Harris, M.; Wu, J. F.; Floyd, R. A.; Butterfield, D. A. A Model for Beta-Amyloid Aggregation and Neurotoxicity Based on Free Radical Generation by the Peptide: Relevance to Alzheimer Disease. *Proc. Natl. Acad. Sci. U.S.A.* **1994**, *91*, 3270−3274.

(4) Butterfield, D. A.; Martin, L.; Carney, J. M.; Hensley, K. Aβ(25−35) Peptide Displays H_2O_2-Like Reactivity toward Aqueous Fe^{2+}, Nitroxide Spin Probes, and Synaptosomal Membrane Proteins. *Life Sci.* **1996**, *58*, 217−228.

(5) Butterfield, D. A. β-Amyloid-Associated Free Radical Oxidative Stress and Neurotoxicity: Implications for Alzheimer's Disease. *Chem. Res. Toxicol.* **1997**, *10*, 495−506.

(6) Fay, D. S.; Fluet, A.; Johnson, C. J.; Link, C. D. In Vivo Aggregation of β-Amyloid Peptide Variants. *J. Neurochem.* **1998**, *71*, 1616−1625.

(7) Panasenko, O. M.; Nova, T. V.; Azizova, O. A.; Vladimirov, Y. A. Free Radical Modification of Lipoproteins and Cholesterol Accumulation in Cells upon Atherosclerosis. *Free Radicals Biol. Med.* **1991**, *10*, 137−148.

(8) Steinberg, D. Antioxidants and Atherosclerosis. A Current Assessment. *Circulation* **1991**, *84*, 1421−1425.

(9) Janero, D. R. Therapeutic Potential of Vitamin E in the Pathogenesis of Spontaneous Atherosclerosis. *Free Radicals Biol. Med.* **1991**, *11*, 129−144.

(10) Hodis, H. N.; Mack, W. J.; LaBree, L.; Cashin-Hemphill, L.; Sevanian, A.; Johnson, R.; Azen, S. Serial Coronary Angiographic Evidence That Antioxidant Vitamin Intake Reduces Progression of Coronary Artery Atherosclerosis. *JAMA, J. Am. Med. Assoc.* **1995**, *273*, 1849−1854.

(11) Boyd, N. F.; McGuire, V. The Possible Role of Lipid Peroxidation in Breast Cancer Risk. *Free Radicals Biol. Med.* **1991**, *10*, 185−190.

(12) Nelson, R. L. Dietary Iron and Colorectal Cancer Risk. *Free Radicals Biol. Med.* **1992**, *12*, 161−168.

(13) Knekt, P.; Reunanen, A.; Takkunen, H.; Aromaa, A.; Heliovaara, M.; Hakuunen, T. Body Iron Stores and Risk of Cancer. *Int. J. Cancer* **1994**, *56*, 379−382.

(14) Omenn, G. S.; Goodman, G. E.; Thornquist, M. D.; Balmes, J.; Cullen, M. R.; Glass, A.; Keogh, J. P.; Meyskens, F. L., Jr.; Valanis, B.; Williams, J. H., Jr.; Barnhart, S.; Hammar, S. Effects of a Combination of Beta Carotene and Vitamin A on Lung Cancer and Cardiovascular Disease. *N. Engl. J. Med.* **1996**, *334*, 1150−1155.

(15) Riemersma, R. A.; Wood, D. A.; Macintyre, C. C. A.; Elton, R. A.; Gey, K. F.; Oliver, M. F. Risk of Angina Pectoris and Plasma Concentrations of Vitamins A, C, and E and Carotene. *Lancet* **1991**, *337*, 1−5.

(16) Salonen, J. T.; Nyyssoner, K.; Korpela, H.; Tuomilehto, J.; Seppanen, R.; Salonen, R. High Stored Iron Levels Are Associated with Excess Risk of Myocardial Infarction in Eastern Finnish Men. *Circulation* **1992**, *86*, 803−811.

(17) Street, D. A.; Comstock, G.; Salkeldy, R.; Klag, M. Serum Antioxidants and Myocardial Infarction. Are Low Levels of Carotenoids and Alpha-Tocopherol Risk Factors for Myocardial Infarction? *Circulation* **1994**, *90*, 1154−1161.

(18) Kushi, L. H.; Folsom, A. R.; Prineas, R. J.; Mink, P. J.; Wu, Y.; Bostick, R. Dietary Antioxidant Vitamins and Death from Coronary Heart Disease in Postmenopausal Women. *N. Engl. J. Med.* **1996**, *334*, 1156−1162.

(19) Stephens, N. G.; Parsons, A.; Schofield, P. M.; Kelly, F.; Cheesman, K.; Mitchisnon, M. J.; Brown, M. J. Randomised Controlled Trial of Vitamin E in Patients with Coronary Disease: Cambridge Heart Antioxidant Study (CHAOS). *Lancet* **1996**, *347*, 781−786.

(20) Krinsky, N. I.; Yeum, K.-J. Carotenoid−Radical Interactions. *Biochem. Biophys. Res. Commun.* **2003**, *305*, 754−760.

(21) Edge, R.; McGarvey, D. J.; Truscott, T. G. The Carotenoids as Antioxidants—A Review. *J. Photochem. Photobiol., B* **1997**, *41*, 189−200.

(22) Goodwin, T. W. Metabolism, Nutrition, and Function of Carotenoids. *Annu. Rev. Nutr.* **1986**, *6*, 273−297.

(23) Kopsell, D. A.; Kopsell, D. E. Accumulation and Bioavailability of Dietary Carotenoids in Vegetable Crops. *Trends Plant Sci.* **2006**, *10*, 499−507.
(24) Fernández-García, E.; Carvajal-Lérida, I.; Jarén-Galán, M.; Garrido-Fernández, J.; Pérez-Gálvez, A.; Hornero-Méndez, D. Carotenoids Bioavailability from Foods: from Plant Pigments to Efficient Biological Activities. *Food Res. Int.* **2012**, *46*, 438−450.
(25) von Lintig, J. Metabolism of Carotenoids and Retinoids Related to Vision. *J. Biol. Chem.* **2012**, *287*, 1627−1634.
(26) Blomhoff, R.; Blomhoff, H. K. Overview of Retinoid Metabolism and Function. *J. Neurobiol.* **2006**, *66*, 606−630.
(27) Li, H.; Tsao, R.; Deng, Z. Factors Affecting the Antioxidant Potential and Health Benefits of Plant Foods. *Can. J. Plant Sci.* **2012**, *92*, 1101−1111.
(28) Rodriguez-Amaya, D. B.; Kimura, M. *Harvestplus Handbook for Carotenoid Analysis*; HarvestPlus Technical Monograph 2; International Food Policy Research Institute (IFPRI) and International Center for Tropical Agriculture (CIAT): Washington, DC, 2004.
(29) Meléndez-Martínez, A. J.; Vicario, I. M.; Heredia, F. J. Effect of Ascorbic Acid on Deterioration of Carotenoids and Colour in Ultrafrozen Orange Juice. *J. Food Compos. Anal.* **2009**, *22*, 295−302.
(30) Crouzet, J.; Kanasawud, P.; Sakho, M. Thermal Generation of Carotenoid-Derived Compounds. *ACS Symp. Ser.* **2002**, *802*, 115−129.
(31) Frank, H. A.; Brudvig, G. W. Redox Functions of Carotenoids in Photosynthesis. *Biochemistry* **2004**, *43*, 8607−8615.
(32) Li, H.; Deng, Z.; Liu, R.; Loewen, S.; Tsao, R. Ultra-Performance Liquid Chromatographic Separation of Geometric Isomers of Carotenoids and Antioxidant Activities of 20 Tomato Cultivars and Breeding Lines. *Food Chem.* **2012**, *132*, 508−517.
(33) Chandler, L. A.; Schwartz, S. J. Isomerization and Losses of *trans* β-Carotene in Sweet Potatoes as Affected by Processing Treatments. *J. Agric. Food Chem.* **1988**, *36*, 129−133.
(34) von E. Doering, W.; Sotiriu-Leventis, C.; Roth, W. R. Thermal Interconversions among 15-*cis*-, 13-*cis*-, and All-*trans*-β-Carotene: Kinetics, Arrhenius Parameters, Thermochemistry, and Potential Relevance to Anticarcinogenicity of All-*trans*-β-Carotene. *J. Am. Chem. Soc.* **1995**, *117*, 2747−2757.
(35) Updike, A. A.; Schwartz, S. J. Thermal Processing of Vegetables Increases *Cis* Isomers of Lutein and Zeaxanthin. *J. Agric. Food Chem.* **2003**, *51*, 6184−6190.
(36) Achir, N.; Randrianatoandro, V. A.; Bohuon, P.; Laffargue, A.; Avallone, S. Kinetic Study of Beta-Carotene and Lutein Degradation in Oils during Heat Treatment. *Eur. J. Lipid Sci. Technol.* **2010**, *112*, 349−361.
(37) Khoo, H.-E.; Prasad, P.; Kong, K.-W.; Jiang, Y.; Ismail, A. Carotenoids and Their Isomers: Color Pigments in Fruits and Vegetables. *Molecules* **2011**, *16*, 1710−1738.
(38) Aparicio-Ruiz, R.; Gandul-Rojas, B. Thermal Degradation Kinetics of Neoxanthin, Violaxanthin, and Antheraxanthin in Virgin Olive Oils. *J. Agric. Food Chem.* **2012**, *60*, 5180−5191.
(39) Aparicio-Ruiz, R.; Minguez-Mosquera, Ma. I.; Gandul-Rojas, B. Thermal Degradation Kinetics of Lutein, β-Carotene and β-Cryptoxanthin in Virgin Olive Oils. *J. Food Compos. Anal.* **2011**, *24*, 811−820.
(40) Falconer, M. E.; Fishwick, M. J.; Land, D. G.; Sayer, E. R. Carotene Oxidation and off-Flavour Development in Dehydrated Carrot. *J. Sci. Food Agric.* **1964**, *15*, 897−901.
(41) Glória, M. B. A.; Grulke, E. A.; Gray, J. I. Effect of Type of Oxidation on Beta-Carotene Loss and Volatile Products Formation in Model Systems. *Food Chem.* **1993**, *46*, 401−406.
(42) Mueller, L.; Boehm, V. Antioxidant Activity of β-Carotene Compounds in Different in Vitro Assays. *Molecules* **2011**, *16*, 1055−1069.
(43) Gentili, A.; Caretti, F. Evaluation of a Method Based on Liquid Chromatography−Diode Array Detector−Tandem Mass Spectrometry for a Rapid and Comprehensive Characterization of the Fat-Soluble Vitamin and Carotenoid Profile of Selected Plant Foods. *J. Chromatogr., A* **2011**, *1218*, 684−697.
(44) Britton, G. UV/Visible Spectroscopy. In *Carotenoids*; Britton, G., Liaanen-Jensen, S., Pfander, H., Eds.; Birkhäuser Verlag: Basel, Switzerland, 1996; Vol. *1B*, pp 13−62.
(45) Gao, Y.; Konovalova, T. A.; Lawrence, J. N.; Smitha, M. A.; Nunley, J.; Schad, R.; Kispert, L. D. Interaction of Carotenoids and Cu^{2+} in Cu-MCM-41: Distance-Dependent Reversible Electron Transfer. *J. Phys. Chem. B* **2003**, *107*, 2459−2465.
(46) Polyakov, N. E.; Focsan, A. L.; Bowman, M. K.; Kispert, L. D. Free Radical Formation in Novel Carotenoid Metal Ion Complexes of Astaxanthin. *J. Phys. Chem. B* **2010**, *114*, 16968−16977.
(47) Hernandez-Marin, E.; Barbosa, A.; Martínez, A. The Capacity of Astaxanthin for Chelating Metal Cations. Does This Have Any Influence on Antiradical Activity? *Molecules* **2012**, *17*, 1039−1054.
(48) Becke, A. D. Density-Functional Thermochemistry. III. The Role of Exact Exchange. *J. Chem. Phys.* **1993**, *98*, 5648−5652.
(49) Stephens, P. J.; Devlin, F. J.; Chabalowski, C. F.; Frisch, M. J. Ab Initio Calculation of Vibrational Absorption and Circular Dichroism Spectra Using Density Functional Force Fields. *J. Phys. Chem.* **1994**, *98*, 11623−11627.
(50) Cancès, M. T.; Mennucci, B.; Tomasi, J. A New Integral Equation Formalism for the Polarizable Continuum Model: Theoretical Background and Applications to Isotropic and Anisotropic Dielectrics. *J. Chem. Phys.* **1997**, *107*, 3032.
(51) Tomasi, J.; Mennucci, B.; Cancès, E. The IEF Version of the PCM Solvation Method: an Overview of a New Method Addressed to Study Molecular Solutes at the QM ab Initio Level. *J. Mol. Struct.: THEOCHEM* **1999**, *464*, 211.
(52) Frisch, M. J.; Trucks, G. W.; Schlegel, H. B.; Scuseria, G. E.; Robb, M. A.; Cheeseman, J. R.; Scalmani, G.; Barone, V.; Mennucci, B.; Petersson, G. A.; et al.; *Gaussian 09*, revision A.08; Gaussian, Inc.: Wallingford CT, 2009.
(53) Yanai, T.; Tew, D.; Handy, N. A New Hybrid Exchange-Correlation Functional Using the Coulomb-Attenuating Method (CAM-B3LYP). *Chem. Phys. Lett.* **2004**, *393*, 51−57.
(54) Boileau, T. W.-M.; Boileau, A. C.; Erdman, J. W., Jr. Bioavailability of All-*trans* and *cis*-Isomers of Lycopene. *Exp. Biol. Med.* **2002**, *227*, 914−919.
(55) Østerlie, M.; Bjerkeng, B.; Liaaen-Jensen, S. Accumulation of Astaxanthin All-E, 9Z and 13Z Geometrical Isomers and 3 and 3′*RS* Optical Isomers in Rainbow Trout (*Oncorhynchus mykiss*) Is Selective. *J. Nutr.* **1999**, *129*, 391−398.
(56) Qiu, D.; Wu, Y.-C.; Zhu, W.-L.; Yin, H.; Yi, L.-T. Identification of Geometrical Isomers and Comparison of Different Isomeric Samples of Astaxanthin. *J. Food Sci.* **2012**, *77*, C934−C940.
(57) Pénicaud, C.; Achir, N.; Dhuique-Mayer, C.; Dornier, M.; Bohuon, P. Degradation of β-carotene during Fruit and Vegetable Processing or Storage: Reaction Mechanisms and Kinetic Aspects: a Review. *Fruits* **2011**, *66*, 417−440.
(58) Chasse, G. A.; Mak, M. L.; Deretey, E.; Farkas, I.; Torday, L. L.; Papp, J. G.; Sarma, D. S. R.; Agarwal, A.; Chakravarthi, S.; Agarwal, S.; Rao, A. V. An Ab Initio Computational Study on Selected Lycopene Isomers. *J. Mol. Struct.: THEOCHEM* **2001**, *571*, 27−37.
(59) Lambelet, P.; Richelle, M.; Bortlik, K.; Franceschi, F.; Giori, A. M. Improving the Stability of Lycopene Z-Isomers in Isomerised Tomato Extracts. *Food Chem.* **2009**, *112*, 156−161.
(60) Cano, M. P.; Marín, M. A. Pigment Composition and Color of Frozen and Canned Kiwi Fruit Slices. *J. Agric. Food Chem.* **1992**, *40*, 2141−2146.
(61) Galano, A. Relative Antioxidant Efficiency of a Large Series of Carotenoids in Terms of One Electron Transfer Reactions. *J. Phys. Chem. B* **2007**, *111*, 12898−12908.
(62) Martínez, A.; Rodríguez-Girones, M. A.; Barbosa, A.; Costas, M. Donator Acceptor Map for Carotenoids, Melatonin and Vitamins. *J. Phys. Chem. A* **2008**, *112*, 9037−9042.
(63) Martínez, A.; Vargas, R.; Galano, A. What Is Important to Prevent Oxidative Stress? A Theoretical Study on Electron-Transfer Reactions between Carotenoids and Free Radicals. *J. Phys. Chem. B* **2009**, *113*, 12113−12120.

(64) Mortensen, A. Scavenging of Benzylperoxyl Radicals by Carotenoids. *Free Radical Res.* **2002**, *36*, 211−216.
(65) Chen, C.-H.; Han, R.-M.; Liang, R.; Fu, L.-M.; Wang, P.; Ai, X.-C.; Zhang, J.-P.; Skibsted, L. H. Direct Observation of the *β*-Carotene Reaction with Hydroxyl Radical. *J. Phys. Chem. B* **2011**, *115*, 2082−2089.
(66) Galano, A.; Vargas, R.; Martínez, A. Carotenoids Can Act as Antioxidants by Oxidizing the Superoxide Radical Anion. *Phys. Chem. Chem. Phys.* **2010**, *12*, 193−200.
(67) Liu, X.; Osawa, T. *Cis* Astaxanthin and Especially 9-*cis* Astaxanthin Exhibits a Higher Antioxidant Activity *in Vitro* Compared to the All-*trans* Isomer. *Biochem. Biophys. Res. Commun.* **2007**, *357*, 187−193.
(68) Levin, G.; Mokady, S. Antioxidant Activity of 9-*cis* Compared to All-*trans β*-Carotene *in Vitro*. *Free Radicals Biol. Med.* **1994**, *17*, 77−82.
(69) Cerezo, J.; Zuñiga, J.; Bastida, A.; Requena, A.; Ceroń-Carrasco, J. P.; Eriksson, L. A. Antioxidant Properties of *β*-Carotene Isomers and Their Role in Photosystems: Insights from Ab Initio Simulations. *J. Phys. Chem. A* **2012**, *116*, 3498−3506.
(70) Martins, J. B. L.; Duraes, J. A.; Sales, M. J. A.; Vilela, A. F. A.; Silve, G. M. E.; Gargano, R. Theoretical Investigation of Carotenoid Ultraviolet Spectra. *Int. J. Quantum Chem.* **2009**, *109*, 739−745.
(71) He, Z.; Sundström, V.; Pullertis, T. Excited States of Carotenoid in LH2: an Ab Initio Study. *Chem. Phys. Lett.* **2001**, *334*, 159−167.
(72) Orian, L.; Carlotto, S.; Di Valentin, M.; Polimeno, A. Charge Transfer in Model Bioinspired Carotene−Porphyrin Dyad. *J. Phys. Chem. A* **2012**, *116*, 3926−3933.
(73) Zhao, L.; Chen, F.; Zhao, G.; Wang, Z.; Liao, X.; Hu, X. Isomerization of *trans*-Astaxanthin Induced by Copper(II) Ion in Ethanol. *J. Agric. Food Chem.* **2005**, *53*, 9620−9623.
(74) Edge, R.; Land, E. J.; McGarvey, D.; Mulroy, L.; Truscott, T. G. Relative One-Electron Reduction Potentials of Carotenoid Radical Cations and the Interactions of Carotenoids with the Vitamin E Radical Cation. *J. Am. Chem. Soc.* **1998**, *120*, 4087−4090.
(75) Cvetkovic, D.; Markovic, D. Stability of Carotenoids toward UV-Irradiation in Hexane Solution. *J. Serb. Chem. Soc.* **2008**, *73*, 15−27.